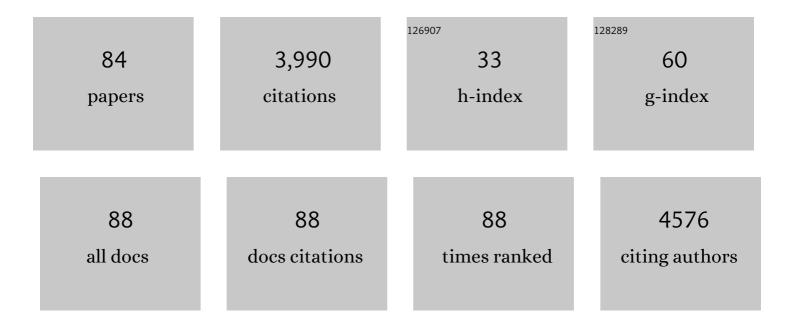
Mary A Mclean

List of Publications by Year in descending order

Source: https://exaly.com/author-pdf/4192316/publications.pdf Version: 2024-02-01



#	Article	IF	CITATIONS
1	Enhancing the spatial resolution of hyperpolarized carbonâ€13 MRI of human brain metabolism using structure guidance. Magnetic Resonance in Medicine, 2022, 87, 1301-1312.	3.0	8
2	Hyperpolarised 13C-MRI identifies the emergence of a glycolytic cell population within intermediate-risk human prostate cancer. Nature Communications, 2022, 13, 466.	12.8	27
3	Hyperpolarized 13C-Pyruvate Metabolism as a Surrogate for Tumor Grade and Poor Outcome in Renal Cell Carcinoma—A Proof of Principle Study. Cancers, 2022, 14, 335.	3.7	18
4	Sodium accumulation in breast cancer predicts malignancy and treatment response. British Journal of Cancer, 2022, 127, 337-349.	6.4	13
5	Magnetization transfer imaging of ovarian cancer: initial experiences of correlation with tissue cellularity and changes following neoadjuvant chemotherapy. BJR Open, 2022, 4, .	0.6	Ο
6	Deuterium metabolic imaging and hyperpolarized 13C-MRI of the normal human brain at clinical field strength reveals differential cerebral metabolism. NeuroImage, 2022, 257, 119284.	4.2	27
7	Imaging Glioblastoma Metabolism by Using Hyperpolarized [1- ¹³ C]Pyruvate Demonstrates Heterogeneity in Lactate Labeling: A Proof of Principle Study. Radiology Imaging Cancer, 2022, 4, .	1.6	17
8	Characterization and correction of centerâ€frequency effects in Xâ€nuclear eddy current compensations on a clinical MR system. Magnetic Resonance in Medicine, 2021, 85, 2370-2376.	3.0	7
9	Investigating the relationship between diffusion kurtosis tensor imaging (DKTI) and histology within the normal human brain. Scientific Reports, 2021, 11, 8857.	3.3	7
10	Combined ²³ Na and ¹³ C imaging at 3.0ÂTesla using a singleâ€ŧuned large FOV birdcage coil. Magnetic Resonance in Medicine, 2021, 86, 1734-1745.	3.0	5
11	Multiparametric MRI of early tumor response to immune checkpoint blockade in metastatic melanoma. , 2021, 9, e003125.		13
12	Hyperpolarized Carbon-13 MRI for Early Response Assessment of Neoadjuvant Chemotherapy in Breast Cancer Patients. Cancer Research, 2021, 81, 6004-6017.	0.9	25
13	Molecular imaging of the prostate: Comparing total sodium concentration quantification in prostate cancer and normal tissue using dedicated ¹³ C and ²³ Na endorectal coils. Journal of Magnetic Resonance Imaging, 2020, 51, 90-97.	3.4	9
14	Fumarate Metabolic Signature for the Detection of Reed Syndrome in Humans. Clinical Cancer Research, 2020, 26, 391-396.	7.0	11
15	Multi-site benchmarking of clinical 13C RF coils at 3T. Journal of Magnetic Resonance, 2020, 318, 106798.	2.1	10
16	Hyperpolarized ¹³ C MRI of Tumor Metabolism Demonstrates Early Metabolic Response to Neoadjuvant Chemotherapy in Breast Cancer. Radiology Imaging Cancer, 2020, 2, e200017.	1.6	40
17	Magnetic resonance fingerprinting of the pancreas at 1.5ÂT and 3.0ÂT. Scientific Reports, 2020, 10, 17563.	3.3	12
18	Hyperpolarized ¹³ C MRI: A novel approach for probing cerebral metabolism in health and neurological disease. Journal of Cerebral Blood Flow and Metabolism, 2020, 40, 1137-1147.	4.3	49

#	Article	IF	CITATIONS
19	Creating a clinical platform for carbonâ€13 studies using the sodiumâ€23 and proton resonances. Magnetic Resonance in Medicine, 2020, 84, 1817-1827.	3.0	24
20	Visualization of sodium dynamics in the kidney by magnetic resonance imaging in a multi-site study. Kidney International, 2020, 98, 1174-1178.	5.2	17
21	Imaging breast cancer using hyperpolarized carbon-13 MRI. Proceedings of the National Academy of Sciences of the United States of America, 2020, 117, 2092-2098.	7.1	138
22	Diffusion kurtosis MRI as a predictive biomarker of response to neoadjuvant chemotherapy in high grade serous ovarian cancer. Scientific Reports, 2019, 9, 10742.	3.3	10
23	Quantifying normal human brain metabolism using hyperpolarized [1–13C]pyruvate and magnetic resonance imaging. NeuroImage, 2019, 189, 171-179.	4.2	144
24	Multi-parametric and multi-regional histogram analysis of MRI: modality integration reveals imaging phenotypes of glioblastoma. European Radiology, 2019, 29, 4718-4729.	4.5	17
25	Sodium MRI with 3D-cones as a measure of tumour cellularity in high grade serous ovarian cancer. European Journal of Radiology Open, 2019, 6, 156-162.	1.6	12
26	Feasibility of Quantitative Magnetic Resonance Fingerprinting in Ovarian Tumors for T ₁ and T ₂ Mapping in a PET/MR Setting. IEEE Transactions on Radiation and Plasma Medical Sciences, 2019, 3, 509-515.	3.7	13
27	Low perfusion compartments in glioblastoma quantified by advanced magnetic resonance imaging and correlated with patient survival. Radiotherapy and Oncology, 2019, 134, 17-24.	0.6	15
28	Non-invasive assessment of glioma microstructure using VERDICT MRI: correlation with histology. European Radiology, 2019, 29, 5559-5566.	4.5	27
29	Measuring tissue sodium concentration: Crossâ€vendor repeatability and reproducibility of ²³ Naâ€MRI across two sites. Journal of Magnetic Resonance Imaging, 2019, 50, 1278-1284.	3.4	17
30	Multi-site repeatability and reproducibility of MR fingerprinting of the healthy brain at 1.5 and 3.0â€⊤. NeuroImage, 2019, 195, 362-372.	4.2	67
31	Hyperpolarized carbon-13 magnetic resonance spectroscopic imaging: a clinical tool for studying tumour metabolism. British Journal of Radiology, 2018, 91, 20170688.	2.2	20
32	lmaging intralesional heterogeneity of sodium concentration in multiple sclerosis: Initial evidence from 23 Na-MRI. Journal of the Neurological Sciences, 2018, 387, 111-114.	0.6	10
33	Diagnostic evaluation of magnetization transfer and diffusion kurtosis imaging for prostate cancer detection in a re-biopsy population. European Radiology, 2018, 28, 3141-3150.	4.5	31
34	Quantification of Total and Intracellular Sodium Concentration in Primary Prostate Cancer and Adjacent Normal Prostate Tissue With Magnetic Resonance Imaging. Investigative Radiology, 2018, 53, 450-456.	6.2	28
35	Quantitative and textural analysis of magnetization transfer and diffusion images in the early detection of brain metastases. Magnetic Resonance in Medicine, 2017, 77, 1987-1995.	3.0	9
36	Assessment of early treatment response to neoadjuvant chemotherapy in breast cancer using non-mono-exponential diffusion models: a feasibility study comparing the baseline and mid-treatment MRI examinations. European Radiology, 2017, 27, 2726-2736.	4.5	51

#	Article	IF	CITATIONS
37	Detecting gasâ€induced vasomotor changes via blood oxygenation levelâ€dependent contrast in healthy breast parenchyma and breast carcinoma. Journal of Magnetic Resonance Imaging, 2016, 44, 335-345.	3.4	3
38	Multiâ€institutional validation of a novel textural analysis tool for preoperative stratification of suspected thyroid tumors on diffusionâ€weighted MRI. Magnetic Resonance in Medicine, 2016, 75, 1708-1716.	3.0	50
39	A comparison of quantitative methods for clinical imaging with hyperpolarized ¹³ Câ€pyruvate. NMR in Biomedicine, 2016, 29, 387-399.	2.8	83
40	Multimodal MRI can identify perfusion and metabolic changes in the invasive margin of glioblastomas. Journal of Magnetic Resonance Imaging, 2016, 43, 487-494.	3.4	41
41	Effect of Radiofrequency Transmit Field Correction on Quantitative Dynamic Contrast-enhanced MR Imaging of the Breast at 3.0 T. Radiology, 2016, 279, 368-377.	7.3	17
42	Relationship Between Brain Glutamate Levels and Clinical Outcome in Individuals at Ultra High Risk of Psychosis. Neuropsychopharmacology, 2014, 39, 2891-2899.	5.4	76
43	3T diffusion-weighted MRI of the thyroid gland with reduced distortion: preliminary results. British Journal of Radiology, 2013, 86, 20130022.	2.2	15
44	Advanced Ovarian Cancer: Multiparametric MR Imaging Demonstrates Response- and Metastasis-specific Effects. Radiology, 2012, 263, 149-159.	7.3	89
45	Slice-selective broadband refocusing pulses for the robust generation of crushed spin-echoes. Journal of Magnetic Resonance, 2012, 223, 129-137.	2.1	8
46	Repeatability of edited lactate and other metabolites in astrocytoma at 3T. Journal of Magnetic Resonance Imaging, 2012, 36, 468-475.	3.4	9
47	DCE and DW MRI in monitoring response to androgen deprivation therapy in patients with prostate cancer: A feasibility study. Magnetic Resonance in Medicine, 2012, 67, 778-785.	3.0	68
48	Reply to: Hippocampal Glutamate Levels and Striatal Dopamine D2/3 Receptor Occupancy in Subjects at Ultra High Risk of Psychosis. Biological Psychiatry, 2011, 70, e3-e4.	1.3	0
49	Prostate cancer metabolite quantification relative to water in ¹ Hâ€MRSI in vivo at 3 Tesla. Magnetic Resonance in Medicine, 2011, 65, 914-919.	3.0	22
50	Apparent diffusion coefficient and vascular signal fraction measurements with magnetic resonance imaging: feasibility in metastatic ovarian cancer at 3 Tesla. European Radiology, 2010, 20, 491-496.	4.5	59
51	Dynamic contrast-enhanced MRI in ovarian cancer: Initial experience at 3 tesla in primary and metastatic disease. Magnetic Resonance in Medicine, 2010, 63, 1044-1049.	3.0	44
52	Altered Relationship Between Hippocampal Glutamate Levels and Striatal Dopamine Function in Subjects at Ultra High Risk of Psychosis. Biological Psychiatry, 2010, 68, 599-602.	1.3	125
53	Metabolic characterization of primary and metastatic ovarian cancer by ¹ Hâ€MRS in vivo at 3T. Magnetic Resonance in Medicine, 2009, 62, 855-861.	3.0	33
54	Proton MR spectroscopy of metabolite concentrations in temporal lobe epilepsy and effect of temporal lobe resection. Epilepsy Research, 2009, 83, 168-176.	1.6	27

#	Article	IF	CITATIONS
55	Glutamate Dysfunction in People with Prodromal Symptoms of Psychosis: Relationship to Gray Matter Volume. Biological Psychiatry, 2009, 66, 533-539.	1.3	210
56	Magnetic resonance spectroscopy: principles and applications in neurosurgery. British Journal of Neurosurgery, 2009, 23, 5-13.	0.8	20
57	The effect of epileptic seizures on proton MRS visible neurochemical concentrations. Epilepsy Research, 2008, 81, 36-43.	1.6	9
58	Spinal cord spectroscopy and diffusion-based tractography to assess acute disability in multiple sclerosis. Brain, 2007, 130, 2220-2231.	7.6	154
59	Proton magnetic resonance spectroscopy of malformations of cortical development causing epilepsy. Epilepsy Research, 2007, 74, 107-115.	1.6	34
60	The effect of sodium valproate on proton MRS visible neurochemical concentrations. Epilepsy Research, 2007, 74, 215-219.	1.6	19
61	Metabolite changes in early relapsing–remitting multiple sclerosis. Journal of Neurology, 2006, 253, 224-230.	3.6	68
62	Magnetisation transfer ratio of choline is reduced following epileptic seizures. NMR in Biomedicine, 2006, 19, 217-222.	2.8	13
63	Concentrations and magnetization transfer ratios of metabolites in gray and white matter. Magnetic Resonance in Medicine, 2006, 56, 1365-1370.	3.0	23
64	Magnetization transfer effect on human brain metabolites and macromolecules. Magnetic Resonance in Medicine, 2005, 54, 1281-1285.	3.0	12
65	Metabolite Changes in Normal-Appearing Gray and White Matter Are Linked With Disability in Early Primary Progressive Multiple Sclerosis. Archives of Neurology, 2005, 62, 569.	4.5	109
66	Elevated white matter myo-inositol in clinically isolated syndromes suggestive of multiple sclerosis. Brain, 2004, 127, 1361-1369.	7.6	193
67	Discrimination between neurochemical and macromolecular signals in human frontal lobes using short echo time proton magnetic resonance spectroscopy. Faraday Discussions, 2004, 126, 93.	3.2	13
68	Magnetic resonance spectroscopy of cerebral cortex is normal in hereditary hyperekplexia due to mutations in the GLRA1 gene. Movement Disorders, 2003, 18, 1538-1541.	3.9	2
69	A Proton Magnetic Resonance Spectroscopy Study of Metabolites in the Occipital Lobes in Epilepsy. Epilepsia, 2003, 44, 550-558.	5.1	61
70	Proton MRS reveals frontal lobe metabolite abnormalities in idiopathic generalized epilepsy. Neurology, 2003, 61, 897-902.	1.1	107
71	Quantitative 1H MRS imaging 14 years after presenting with a clinically isolated syndrome suggestive of multiple sclerosis. Multiple Sclerosis Journal, 2002, 8, 207-210.	3.0	62
72	Brain metabolite changes in cortical grey and normal-appearing white matter in clinically early relapsing-remitting multiple sclerosis. Brain, 2002, 125, 2342-2352.	7.6	255

#	Article	IF	CITATIONS
73	Reproducibility of in vivo metabolite quantification with proton magnetic resonance spectroscopic imaging. Journal of Magnetic Resonance Imaging, 2002, 15, 219-225.	3.4	43
74	A Short-echo-time Proton Magnetic Resonance Spectroscopic Imaging Study of Temporal Lobe Epilepsy. Epilepsia, 2002, 43, 1021-1031.	5.1	68
75	In Vivo Short Echo Time 1H-Magnetic Resonance Spectroscopic Imaging (MRSI) of the Temporal Lobes. NeuroImage, 2001, 14, 501-509.	4.2	33
76	Quantitative short echo time proton magnetic resonance spectroscopic imaging study of malformations of cortical development causing epilepsy. Brain, 2001, 124, 427-436.	7.6	55
77	Preliminary evidence for neuronal damage in cortical grey matter and normal appearing white matter in short duration relapsing-remitting multiple sclerosis: a quantitative MR spectroscopic imaging study. Journal of Neurology, 2001, 248, 131-138.	3.6	136
78	Quantitative analysis of short echo time1H-MRSI of cerebral gray and white matter. Magnetic Resonance in Medicine, 2000, 44, 401-411.	3.0	145
79	Multimodal MR Imaging: Functional, Diffusion Tensor, and Chemical Shift Imaging in a Patient with Localizationâ€Related Epilepsy. Epilepsia, 1999, 40, 1459-1462.	5.1	54
80	Short echo time single-voxel1H magnetic resonance spectroscopy in magnetic resonance imaging-negative temporal lobe epilepsy: Different biochemical profile compared with hippocampal sclerosis. Annals of Neurology, 1999, 45, 369-376.	5.3	131
81	Absolute metabolite quantification by in vivo NMR spectroscopy: IV. multicentre trial on MRSI localisation tests. Magnetic Resonance Imaging, 1998, 16, 1113-1125.	1.8	15
82	Approaches to Studies on Neuronal/Glial Relationships by ¹³ C-MRS Analysis. Developmental Neuroscience, 1996, 18, 434-442.	2.0	66
83	Continuing Ischemic Damage After Acute Middle Cerebral Artery Infarction in Humans Demonstrated by Short-Echo Proton Spectroscopy. Stroke, 1995, 26, 1007-1013.	2.0	134
84	Magnetic resonance neurography of the median nerve. British Journal of Radiology, 1994, 67, 1169-1172.	2.2	26